Chapter III

Experimental Techniques and Calculations

3.1 Introduction:

In this chapter, the experimental details employed in the characterization of the semiconductor samples will be briefly discussed. The crystalline and amorphous semiconductors were characterized by various techniques. Both the electrical and optical properties of the crystalline and amorphous semiconductors were studied. Section 3.2 briefly describes the technique of X-ray diffraction. The structures of the samples were analyzed using an X-ray-diffractometer. Section 3.3 describes the Four-Point Probe technique used to measure the conductivity of crystalline Ge and the calculation of energy gap of the sample. The conductivity of the Germanium sample was studied using the Scientific Equipment and Services Four Point Probe model DEP-02. Section 3.4 briefly gives the preparation details while section 3.5 gives the dc electrical characterization technique of a-Si:H. Conductivity measurements were carried out on the a-Si:H sample using the Keithley 236 Source Measurement Unit (SMU) in a Janis Research Co., Inc. model CCS 100 cryostat for measurements at liquid nitrogen temperature to 320°K. This section also describes the calculation of conductivity, activation energies, and density of states at the Fermi-level. The conductivity of crystalline Silicon was too low for measurement using the Four-Point Probe. Aluminium electrodes in the transverse configuration were made on the sample by vacuum deposition technique and the conductivity was measured by the direct method, used for a-Si:H. Section 3.6 focuses on the Infrared spectroscopic studies done on Crystalline and amorphous semiconductors to

ascertain the bonding configurations present in the sample and hence the purity of the sample. Section 3.7 describes the optical transmission measurements on crystalline Silicon using the Shimadzu UV-VIS NIR-PC3101 double beam spectrophotometer and optical calculations. The optical characterization using the UV-VIS-NIR spectrophotometer in both the reflectance and transmission mode was not done on the crystalline-Ge since the energy gap is about 0.66eV and the absorption does not occur within this spectral range. Section 3.8 discusses the optical characterization of a-Si:H using the Jasco UV-VIS NIR model 310-PC double beam spectrophotometer and the methods adopted for the calculation of various physical parameters like refractive index, thickness, absorption coefficient and hydrogen content of the sample. Section 3.9 highlights the annealing process carried out on the a-Si:H samples at different temperatures to study the effect of annealing on the optical and electrical properties of a-Si:H.

3.2 Techniques of Characterization of Materials:

3.2.1 X-ray Diffraction:

X-ray diffraction is a versatile, non-destructive analytical technique for identification and quantitative determination of the various crystalline forms, known as 'phases', of compounds present in solid materials and powders. The phenomenon of diffraction occurs when penetrating radiation, such as X-rays, enters a crystalline substance and is scattered. The direction and intensity of the scattered (diffracted) beams depend on the orientation of the crystal lattice with respect to the incident beam. A crystal lattice is a regular three-dimensional distribution (cubic, rhombic, etc.) of atoms in space. These are arranged so that they form a series of parallel planes separated from one another by a distance 'd', which varies according to the nature of the material. For any crystal, planes exist in a number of different orientations - each with its own

specific d-spacing. When a monochromatic X-ray beam with wavelength λ is incident on lattice planes in a crystalline material at an angle θ, diffraction occurs only when the distance travelled by the rays reflected from successive planes differs by a complete number n of wavelengths, the relation between θ and 'n' is given by Bragg's law

$$n\lambda = 2d\sin\theta \qquad (3.1)$$

By varying the angle ɵ, the Bragg's Law conditions are satisfied by different d-spacing in polycrystalline materials. Plotting the angular positions and intensities of the resultant diffracted peaks of radiation produces a pattern which is characteristic of the sample. Where a mixture of different phases is present, the resultant diffractogram is formed by addition of the individual patterns. The diffractometer in the present study (Philips PW 1840) utilizes a sample holder, a goniometer, and a fixed-position detector to measure the diffraction patterns of unknowns. The goniometer provides a wide range of angle of incidence, and the detector measures the intensity of the diffracted beam. The resulting analysis is

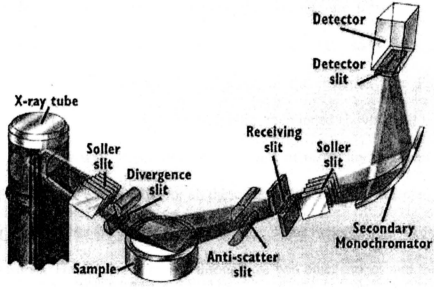

Figure 3.1 Schematic of X-ray diffractometer

described graphically as a set of peaks with % intensity on the Y-axis and goniometer angle on the X-axis.

Parameters	Crystalline Semiconductor	Amorphous Semiconductor
Source	Cu-K_α(λ=1.544□)	Cu-K_α(λ=1.544□)
Voltage	40KV	40KV
Current	30mA	30mA
Scan Type	Continuous	Continuous
Scan step size	0.020 degrees	0.040 degrees
Scan step time	0.20 Sec	1.0 Sec
Range (c.p.s)	10.00-110.00	10.00-60.00

Table 3.1 Configuration used in X-ray diffractometer

3.3 Conductivity Measurement for Crystalline Semiconductor by Four-Point Probe Technique:-

Many conventional methods for the measurement of resistivity of semiconductors are unsatisfactory because metal-semiconductor contacts are usually rectifying in nature. Also usually there is minority carrier injections to the sample by the current carrying contact which changes the resistance of the material. The Four Probe method described here overcomes the difficulties mentioned above and it has several other advantages as well. It permits measurements of resistivity in samples having different shapes. The basic model for all these measurements is represented in Figure 3.2. Four sharp probes are placed on a flat surface of the material whose resistivity is to be measured. The current is passed through the two outer probes and the floating potential is measured across the inner pair. To prevent minority carrier injection and

to make good contacts the surface on which the probe rest should be mechanically

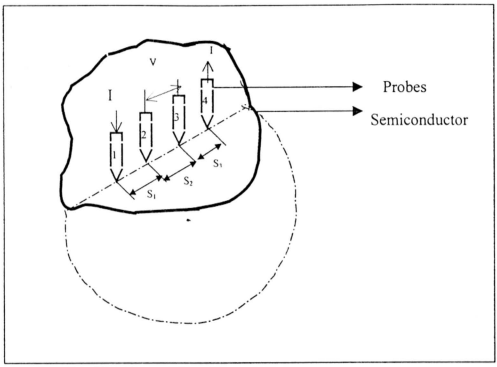

Figure. 3.2 Model for the Four-Probe Resistivity Measurements [48]

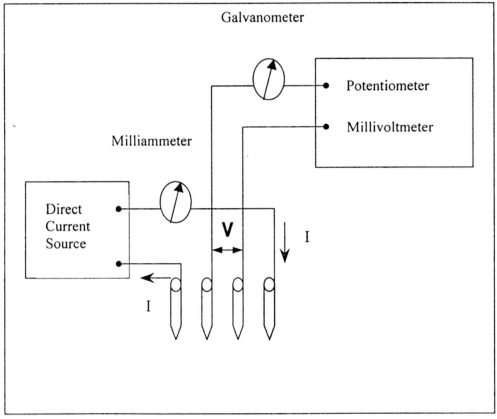

Figure 3.3 Circuit used for Resistivity Measurements

lapped. The experimental circuit used in this measurement is illustrated in Figure 3.3. A nominal value of the probe spacing that is found satisfactory is 2mm between the adjacent probes. This permits measurement with reasonable current on 'n' and 'p' type semiconductor. To use the Four-Probe method, the following assumptions are necessary:-

1. The resistivity of the material under measurement must be uniform
2. If there is minority carrier injection into the sample by the current carrying probe, most of the carriers must recombine near the electrodes so that their effect on the conductivity is negligible.
3. The surfaces on which the probes rest must be flat with no surface leakage.
4. The probes resting on the sample surface must touch it along a straight line.
5. The diameters of the contact of metallic probes and the semiconductor should be small compared to the distance between the probes.

Case I

Resistivity Measurements on a Thick Sample:

We will consider the semiconductors to be of semi-infinite volume as shown in Figure 3.2. Four probes are spaced S_1, S_2, and S_3 apart as shown. Current I is passed through the outer probes (1&4) and the floating potential 'V' is measured across the inner pair of probes (2&3). The floating potential V_f at a distance 'r' from an electrode carrying a current I in a material of resistivity ρ_0 is given by [48]

$$V_f = \frac{\rho_0 I}{2\pi r} \qquad (3.2)$$

In Figure. 3.2 there are two current carrying electrodes numbered 1 & 4. The floating potential V_f at any point within the semiconductor is the difference between the

potentials induced by each of the electrodes since they carry currents of equal magnitudes in opposite directions. Therefore,

$$V_f = \frac{\rho_0 I}{2\pi}\left(\frac{1}{r_1} - \frac{1}{r_4}\right) \qquad (3.3)$$

Where r_1 is the distance from probe 1 and r_4 is the distance from probe 4. Therefore the floating potentials V_{f2} and V_{f3} at probes 2 and 3 respectively can be calculated from equation (3.3) by substituting their distances. The corresponding expressions are ;

$$V_{f2} = \frac{\rho_0 I}{2\pi}\left(\frac{1}{S_1} - \frac{1}{S_2 + S_3}\right)$$

$$V_{f3} = \frac{\rho_0 I}{2\pi}\left(\frac{1}{S_1 + S_2} - \frac{1}{S_3}\right)$$

The potential difference 'V' between probes 2 & 3 is then;

$$V = V_{f2} - V_{f3} = \frac{\rho_0 I}{2\pi}\left(\frac{1}{S_1} + \frac{1}{S_3} - \frac{1}{S_2 + S_3} - \frac{1}{S_1 + S_2}\right)$$

and the resistivity ρ_0 works out as;

$$\rho_0 = \frac{V}{I} \times \frac{2\pi}{\left(\frac{1}{S_1} + \frac{1}{S_3} - \frac{1}{S_1 + S_2} - \frac{1}{S_2 + S_3}\right)} \qquad (3.4)$$

When the point spacing are equal (i.e) $S_1 = S_2 = S_3 = S$, expression (3.4) simplifies to,

$$\rho_0 = \frac{V}{I} 2\pi s \qquad (3.5)$$

Case II

If the specimen cannot be regarded as semi-infinite, corrections to the resistivity values have to be applied. If the bottom surface can be regarded as conducting and parallel to the non-conducting top surface, the corrections to be applied may be deduced as follows. The model for this case is shown in Figure 3.4. The width of the slice is presumed to be 'W'. In the Fig the polarity and spacing of the first few

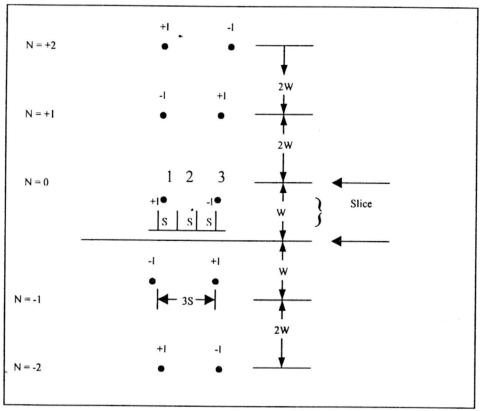

Figure 3.4 Images for the case of the Resistivity Probes on a thin slice with a conducting bottom surface [49]

images have been shown. The floating potential at the electrode two is:

$$V_{f2} = \frac{\rho I}{2\pi}\left[\sum_{n=-\infty}^{n=+\infty}(-1)^n \frac{1}{\sqrt{S^2+(2nw)^2}} - \sum_{n=-\infty}^{n=\infty}(-1)^n \frac{1}{\sqrt{(2S)^2+(2nw)^2}}\right]$$

Similarly, the floating potential V_{f3} at the electrode three is,

$$V_{f3} = \frac{\rho I}{2\pi}\left[\sum_{n=-\infty}^{+\infty}(-1)^n \frac{1}{\sqrt{(2S)^2+(2nw)^2}} - \sum_{n=-\infty}^{+\infty}(-1)^n \frac{1}{\sqrt{(S)^2+(2nw)^2}}\right]$$

Hence $V = V_{f2} - V_{f3}$.

$$V = \frac{\rho I}{2\pi}\left[\sum_{n=-\infty}^{+\infty}(-1)^{n11}\frac{2}{\sqrt{(S)^2+(2nw)^2}} - \sum_{n=-\infty}^{+\infty}(-1)^n\frac{2}{\sqrt{(2S)^2+(2nw)^2}}\right]$$

$$= \frac{\rho I}{2\pi}\left[\frac{1}{S} + \sum_{n=1}^{\infty}(-1)^n\frac{4}{\sqrt{S^2+(2nw)^2}} - \sum_{n=1}^{\infty}(-1)^n\frac{4}{\sqrt{(2S)^2+(2nw)^2}}\right] \qquad (3.6)$$

If the thickness 'w' is infinite equation (3.6) reduces to equation (3.5).

Equation (3.6) can be written as,

$$\rho = \frac{\rho_0}{G\left(\frac{w}{S}\right)} \qquad (3.7)$$

where $\rho_0 = \frac{V}{I} \times 2\pi S$

and,

$$G\left(\frac{w}{S}\right) = 1 + \frac{4S}{w}\sum_{n=1}^{\infty}(-1)^n\left[\frac{1}{\sqrt{\left(\frac{S}{w}\right)^2+(2n)^2}} - \frac{1}{\sqrt{\left(\frac{2S}{w}\right)^2+(2n)^2}}\right] \qquad (3.8)$$

Case III

The model for these measurements is the same as case II except that the bottom surface is non-conducting. This means that all the images of Figure (3.4) have the same charge as the current source. In that case ;

$$\rho = \frac{\rho_0}{G^1\left(\frac{w}{S}\right)} \qquad (3.9)$$

where ,

$$G^{1}\left(\frac{w}{S}\right) = 1 + \frac{4S}{w}\sum_{n=1}^{\infty}\left[\frac{1}{\sqrt{\left(\frac{S}{w}\right)^{2} + (2n)^{2}}} - \frac{1}{\sqrt{\left(\frac{2S}{w}\right)^{2} + (2n)^{2}}}\right] \qquad (3.10)$$

If the specimen is very thin or (S/w) is a large quantity equation (3.10) reduces to;

$$G^{1}\left(\frac{w}{S}\right) = \frac{2S}{w}\ln 2 \qquad (3.11)$$

The corrections G(w/S) and G^{1}(w/S) have been calculated and tabulated in table 3.2. The values of the corrections as a function of (w/S) are plotted in Figure (3.5) and Figure (3.6) respectively. Earlier it was presumed that probes are situated far away from the semiconductor boundary. In case the probes are not situated far from the boundary appropriate finite corrections have to be applied. The finite correction factor 'C' has been tabulated in table 3.3.

S.No	W/S	G_6(W/S)	G_7(W/S)
1	0.100	0.0000019	13.863
2	0.141	0.00018	9.704
3	0.200	0.00342	6.931
4	0.330	0.0604	4.159
5	0.500	0.228	2.780
6	1.000	0.683	1.504
7	1.414	0.848	1.223
8	2.000	0.933	1.094
9	3.333	0.9838	1.0228
10	5.000	0.9948	1.0070
11	10.000	0.9993	1.00045

Table 3.2 Correction Divisor for a thin slice with conducting and non-conducting bottom surface [49]

$\frac{d}{s}$	Circle diameter $\frac{d}{s}$	Square $\frac{a}{d}=1$	Rectangle		
			$\frac{a}{d}=2$	$\frac{a}{d}=3$	$\frac{a}{d}\geq 4$
1.00				0.9988	0.9994
1.25				1.2467	1.2248
1.50			1.4788	1.4893	1.4893
1.75			1.7196	1.7238	1.7238
2.00			1.9475	1.9475	1.9475
2.50			2.3532	2.3541	2.3541
3.00	2.2662	2.4575	2.7000	2.7005	2.7005
4.00	2.9289	3.1137	3.2246	3.2248	3.2248
5.00	3.3625	3.5098	3.5749	3.5750	3.5750
7.50	3.9273	4.0095	4.0361	4.0362	4.0362
10.00	4.1716	4.2209	4.2357	4.2357	4.2357
15.00	4.3646	4.3882	4.3947	4.3947	4.3947
20.00	4.4364	4.4516	4.4553	4.4553	4.4553
40.00	4.5076	4.5120	4.5129	4.5129	4.5129
∞	4.5324	4.5324	4.5325	4.5325	4.5325

Table 3.3 Correction Factor C.F for the measurement of Sheet resistance with the Four-Point Probe [49]

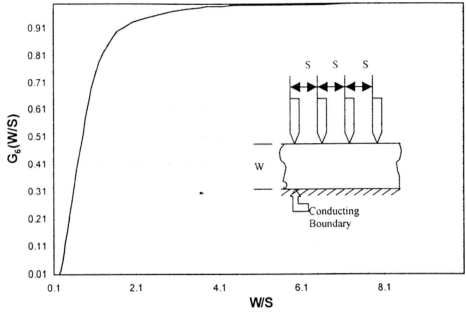

Figure 3.5. Correction Divisor for probes on a slice with a conducting bottom surface. [49]

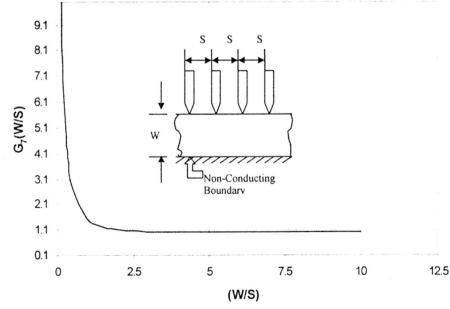

Figure 3.6 Correction Divisor for probes on a thin slice with a non-conducting bottom surface. [49]

3.3.1 Brief description of the Apparatus:-

1. Probes arrangement:-

It has four individually spring loaded probes coated with Zinc at the tips. The probes are collinear and equally spaced. The Zinc coating and individual springs ensures good electrical contacts with the sample. The probes are mounted on a Teflon bush, which ensures a good electrical insulation between the probes. A Teflon spacer near the tips is also provided to keep the probes at equal distances. The whole arrangement is mounted on a suitable stand and leads are provided for voltage and current measurements.

2. Oven:-

The four-Probes are placed in a small oven for the variation of the temperature of the crystal from room temperature to about 200°C.

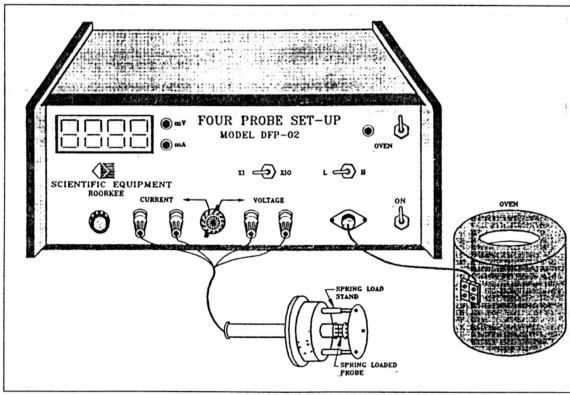

Figure 3.7 A Four-Probe Setup

3. Four-Probe Set-up (Measuring unit):-

It has following three sub-units all enclosed in one cabinet:

a) Multi range digital voltmeter, b) Constant current generator and c) Oven power supply. A Four-Probe setup diagram is given in figure 3.7.

4. Experimental Procedure:-

The sample was put in the base plate of the Four-Probe arrangement. and the continuity between the probes was checked for proper electrical contacts. The outer pair of probes was connected to the constant current generator and the inner pair was connected to the probe voltage terminal. The Four-Probe arrangement was placed within the oven and a thermometer was placed into the oven to measure the temperature of the sample. The current from the constant current generator was adjusted to about 5mA. The power supply to the oven was turned on during the measurement and the variation of the voltage with increasing temperature was noted.

3.3.2 Calculation:-

It has already been proved that (see equation 3.5), $\rho_0 = \frac{V}{I} 2\pi s$. Since, the thickness of the crystal is comparable to probe spacing and other crystal dimensions, correction factors are to be appropriately applied to evaluate the true resistivity of the crystal. Thus ρ may be calculated at various temperatures. Next a graph of $\log_{10}\sigma$ Vs T^{-1} (temperature) is plotted. From the intrinsic part of the slope the E_g was calculated as already discussed in the theory of crystalline semiconductors in chapter II (see equation 2.6).

3.4 Preparation of a-Si:H:-

The a-Si:H samples were plasma deposited from silane on to a quartz substrate by home built horizontal DC-plasma glow discharge system. The deposition parameters were, substrate temperature (T_S) 21°C, power absorbed in the plasma 6.24 watts, silane flow rate 10sccm, base pressure 4.2×10^{-2}mbar. During deposition the pressure rose to 8×10^{-1}mbar. The current during deposition was maintained at 12mA and the deposition potential was maintained at 520volts. The duration of deposition time was 25 minutes. The film was deposited at an average rate of 2 Å/sec and was 0.30μm thick.

3.5 Electrical Characterization of a-Si:H:-

The conductivity of amorphous semiconductors are very low therefore the bulk conductivity of the a-Si:H prepared by plasma glow discharge was measured by making aluminium electrodes on the sample. The conductivity was later measured by Keithley 236 Source Measurement Unit. The various steps followed in the measurement of the conductivity right from making of the aluminium electrode is explained below.

3.5.1 Electrode Deposition:

The purpose of depositing aluminium electrode is to establish electrical contacts. The electrodes were deposited by using the home-built vacuum evaporation system. The source aluminium wires were suspended on a tungsten filament and the filament was held in air directly below the target sample (a-Si:H) by means of a low tension lead-ins. The target sample was placed on an aluminium mask, which rested on the bottom of a cylindrically shaped glass. The evaporation chamber was evacuated by

means of a diffusion pump and a high vacuum valve. The lines were evacuated by Edward's rotary pump. The pressure inside the chamber was maintained at $2x10^{-4}$ mbar and a current of 25-28 Amperes were passed through the filament during deposition. The electrodes were deposited with a separation of approximately 0.02cm-0.03cm on the face of the sample. A schematic representation of the vacuum evaporation system is given in figure 3.10.

3.5.2 D.C Conductivity Measurements:

The Janis Research Co., Inc.. Model CCS 100 Cryostat was used for the conductivity measurement at different temperatures. The cryostat has a thin vacuum jacket, electrical feed through to connect to the Source Measurement Unit (SMU), a

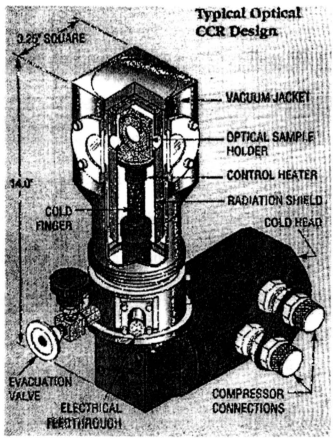

Figure 3.9 The Cold finger Cryostat

pressure relief wall and a sample mount. Just below the sample mount is a sensor to measure the temperature of the sample. The cryostat at the bottom was connected to the Leybold Helium compressor unit. Temperature below 78K was achieved by using a vacuum pump and the Helium compressor. The Cryostat is shown in the figure 3.9. A steady temperature throughout the measurement was achieved with Lake Shore 330 autotuning temperature controller.

The sample was mounted carefully into the cryostat and was fixed to the sample holder by screws. The screws were tightened to ensure good electrical contacts. The connection between the sample, cryostat and the SMU was made by connecting two thin insulated copper wires to the electrodes of the sample by means of silver paste and the other end of the wires were soldered to the electrical pin that is around the middle of the cryostat. Initially the cryostat was evacuated to a pressure of $6\chi10^{-2}$ mbar and then the helium compressor was turned on to cool down the sample. Current-voltage measurements were made at fixed temperature by using Keithley 236-source measurement unit (SMU) supported by Metrics computer software. The current-voltage measurement of the a-Si:H film were carried out at different temperatures between 77°K-320°K. Finally, d.c conductivity at these temperatures were calculated and $\ln\sigma$ as a function of inverse absolute temperature was plotted. From the graph the activation energy at different states were calculated. Before making the above current-voltage measurements the sample was subjected to a constant voltage of 100volts for several hours by using the time measure mode of the Metrics software. This process is known as empty trap and is used to eliminate traps in the sample. A diagram of the electrical circuitry for current-voltage measurement is given in the figure 3.11 Table 3.4 gives the configuration used in the SMU during

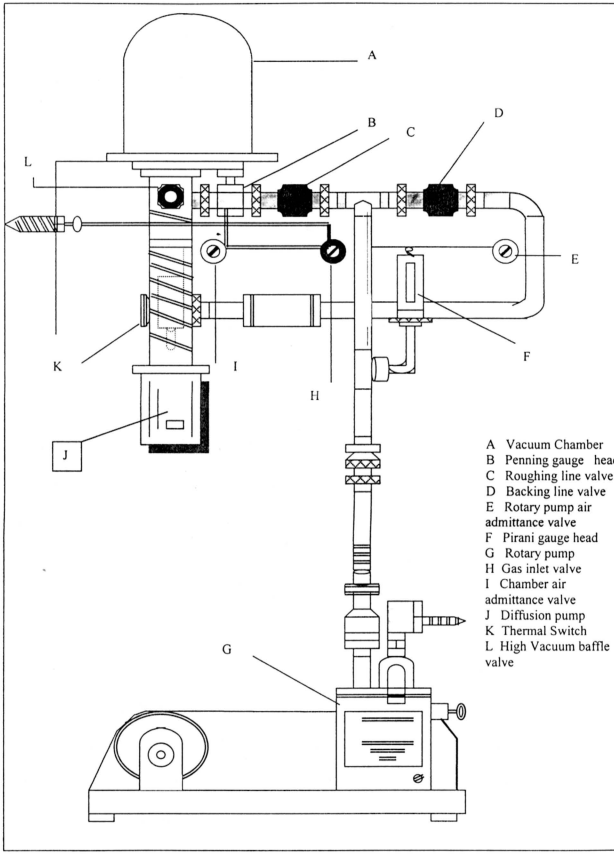

Figure 3.10 A Sketch of the Vacuum evaporation system [50]

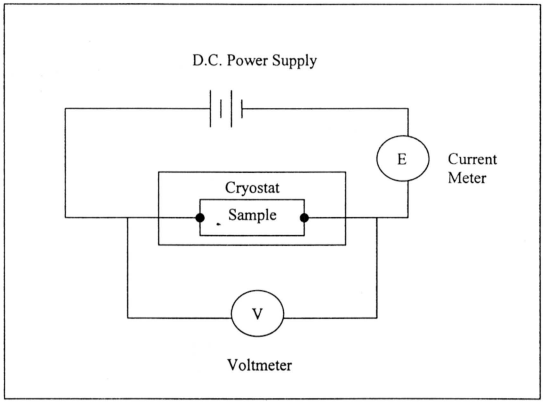

Figure 3.11 Electrical circuitry for current-voltage measurement

measurement. And the table 3.5 gives the configuration used in the SMU during empty trap. Since the conductivity of crystalline-Si could not be measured by Four-Point Probe, electrodes were made on the top and bottom surface of the sample as mentioned in section 3.4.1. The DC conductivity of the crystalline-Si was measured using the VPF 100 Cryostat and 236 Keithley source measurement unit. And the current-voltage measurement was carried on between 300-430K. The Lake Shore 320 autotuning temperature controller was used throughout the measurement. The configurations used in the SMU during current voltage measurement for Crystalline-Si is given in table 3.6. Before all measurements care should be taken to turn off the pump and should make sure that

the gas inlet is closed to avoid up surging of oil into the cryostat. It is necessary to turn on the power supply to the temperature controller, SMU and computer at least

half-an hour before making measurements in order to warm up the system. Before all measurements a constant voltage of 100 volts was applied to the sample for at least two hours reversing the polarity in an hour interval to elevate the electrons trapped in the mobility gap.

Mode	Sweep
Type	Linear
Measure	Voltage and Current
Start	0 volts
Stop	100 volts
No: of points	201
Interval	0.5 volts
Time delay	0
Integration	50Hz
Filter	4 reading

Table 3.4 Configuration used in the SMU during sweep mode for a-Si:H

Mode	Constant
Type	Linear
Stimulus	Voltage
Measure	Current
Value	100volts
Delay	0
Integration	50Hz
Filter	1 reading

Table 3.5.Configurations used in SMU during empty trap for a-Si:H

Mode	Sweep
Type	Linear
Measurement	Voltage and Current
Start	0
Stop	100mV
No: of points	201
Interval	500μV
Time delay	0
Integration	50 Hz
Filter	4 readings

Table 3.6 Configurations used in the SMU during current-voltage measurement of Crystalline-Si

3.5.3 Calculation of DC-conductivity:

The conductivity of the sample is calculated using the following expression.

$$\sigma = \frac{I}{V} \cdot \frac{d}{w \times t} \qquad (3.12)$$

where ,I is the current flowing through the electrode, d is the length of the gap, V is the voltage applied across the cross-section, W is the width of the electrode and t is the thickness of the film. (a-Si:H).

Here I/V measures the slope of the I-V curve in the ohmic region. Equation (3.12) can be written in the following form.

$$\sigma = \frac{m.d}{w \times t} \qquad (3.13)$$

Where m = slope of the I-V curve in the ohmic region. The slope is calculated by the least square method that was carried out using the Microsoft Excel software. The ohmic region is identified where the slope of log I verses log V curve is equal to unity.

3.5.4 Calculation of Activation Energies:-

For the calculation of activation energies we made use of $\ln\sigma$ verses 1/T curves. The representative curve to carry out the calculation is shown in fig 2.6. Slope m1 represents the extended state conduction, where the activation energy is given by [equation (2.29)]

$$(E_C\text{-}E_F) = km_1 \qquad (3.14)$$

Where k = Boltzmann's constant = 8.6×10^{-5} eV / deg.k

Slope m_2 represent the conduction in tail state region where it can be used to determine $(E_A\text{-}E_F)$ as ; [equation (2.34)]

$$(E_A\text{-}E_F) = km_2 \qquad (3.15)$$

To find out $(E_C\text{-}E_A)$ we make use of equation (3.14) and equation (3.15)

Which leads to,

$$(E_C\text{-}E_A)=(E_C\text{-}E_F)\text{-}(E_A\text{-}E_F) = k(m_2 - m_1) \qquad (3.16)$$

3.5.5 Calculation of density of states at E_F:-

It was established in equation (2.46) that for amorphous material at low temperatures Mott's treatment of variable range hopping leads to a temperature

$$\sigma = \frac{m.d}{w \times t} \qquad (3.13)$$

Where m = slope of the I-V curve in the ohmic region. The slope is calculated by the least square method that was carried out using the Microsoft Excel software. The ohmic region is identified where the slope of log I verses log V curve is equal to unity.

3.5.4 Calculation of Activation Energies:-

For the calculation of activation energies we made use of lnσ verses 1/T curves. The representative curve to carry out the calculation is shown in fig 2.6. Slope m1 represents the extended state conduction, where the activation energy is given by [equation (2.29)]

$$(E_C\text{-}E_F) = km_1 \qquad (3.14)$$

Where k = Boltzmann's constant = 8.6×10^{-5} eV / deg.k

Slope m_2 represent the conduction in tail state region where it can be used to determine $(E_A\text{-}E_F)$ as ; [equation (2.34)]

$$(E_A\text{-}E_F) = km_2 \qquad (3.15)$$

To find out $(E_C\text{-}E_A)$ we make use of equation (3.14) and equation (3.15)

Which leads to,

$$(E_C\text{-}E_A)=(E_C\text{-}E_F)\text{-}(E_A\text{-}E_F) = k(m_2 - m_1) \qquad (3.16)$$

3.5.5 Calculation of density of states at E_F:-

It was established in equation (2.46) that for amorphous material at low temperatures Mott's treatment of variable range hopping leads to a temperature

dependence for the conductivity of the form $\sigma = \sigma_0(T)\exp\left(\frac{-A}{T^{\frac{1}{4}}}\right)$. The parameter $N(E_F)$ can be evaluated from the slope of a plot of $\ln[\sigma(T)T^{1/2}]$ vs $T^{-1/4}$ and from the intercept at $T^{-1/4}=0$ making a reasonable assumption for ν_{ph} [51].

3.6 Infrared Spectroscopy:

Infrared spectroscopy is a technique applied to know the chemical structure of the sample. The Crystalline and amorphous semiconductor samples were scanned in the range of 370-4000cm^{-1}. The main purpose of the application of this technique is to determine the presence of oxygen in the sample, as the presence of oxygen greatly affects the conductivity of the sample. For the present study, the Perkin Elmer system 2000 FT-IR spectrophotometer was used to analyze the sample. The troughs in the spectrum was characteristic of the constituents of the sample which are detailed in the next chapter.

3.7 Optical Characterization of Crystalline Semiconductor:

3.7.1 UV-VIS Transmission Spectroscopy:

An optical transmission spectrum of Crystalline-Si over a range of 200nm-3000nm was obtained by using a Shimadzu UV-VIS spectrophotometer model UV-3101PC. A schematic block diagram is shown in the figure 3.8. The set-up consists of a light source, a monochromator, a sample compartment (which holds the sample and the reference holder), a photomultiplier tube (which is used as a detector) and a computer to automate the measurement. Firstly, the baseline was obtained by using air as the reference and scanned in the range 200nm-3000nm. Once the base line was

obtained the sample was placed in the sample holder and the transmission spectrum of the sample was obtained by scanning the sample in the same range.

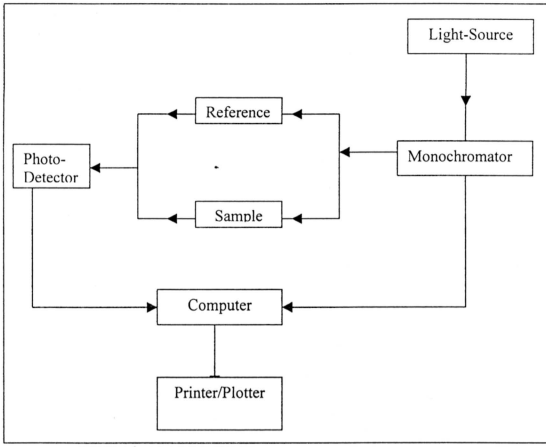

Fig 3.8 A Schematic block diagram of UV-VIS spectrophotometer

3.7.2 Calculation of Refractive index (η), Absorption constant (k) and Coefficient of absorption (α).

The transmission spectrum provided the absorption edge of the sample. When the transmission is nearly equal to one, the refractive index of the sample was obtained by assuming the absorption constant to be equal to zero using the equation (2.8). Once the refractive index was obtained the absorption constant k was calculated for reflectance at each wavelength by using he equation (2.8). Then, the coefficient of absorption (α) was calculated by substituting the appropriate value of k for each

wavelength by using the equation (2.9). Finally, a graph of (α) against (λ) was plotted.

3.8 Optical Characterization of a-Si:H:

3.8.1. Transmission Measurement:

The optical transmission spectrum is indeed a very useful technique in thin film characterization. In this work the transmission spectrum is obtained using a Jasco UV-VIS-NIR 3101-PC double beam spectrophotometer. .A schematic block diagram is already shown in the figure. 3.8. The set-up consists of a light source, a monochromator, a sample compartment, which holds the sample and reference holder, a photomultiplier tube which is used as a detector and a computer to automate the measurements. For this work the scanning range selected was 200nm - 2500nm. Initially, two reference quartz slides similar to the ones used as substrates are placed in the sample holder and scanned in the range of 200nm-2500nm to obtain the baseline. Once the baseline is obtained, one of the quartz slides is replaced with the sample, leaving the other as reference. The transmission spectrum of the sample is then obtained within the same range. A typical transmission spectrum of a-Si:H is shown in figure 3.12. The transmission spectrum is used to obtain the refractive index, thickness of the sample, optical energy gap and hydrogen content of the sample.

3.8.2 Measurement of Refractive index, Thickness of thin films, Absorption Coefficient, and Optical Energy gap.

Measurement of the film thickness is a prerequisite to optical absorption studies. The thickness calculated from optical transmission spectrum is substituted into the

conductivity equation (3.13) to calculate the σ. Measurements of the above parameters of the thin film give some information's about the effect of annealing on the sample. The method proposed by J.G. Manifacier, J. Gasiot and J.P Fillard [52] is used to determine the refractive index and optical thickness of the film. T_{max} and T_{min} are considered as continuous envelope functions of λ in the transmission spectrum, a representative figure is illustrated in figure 3.12. Therefore, by using curve-fitting techniques the continuous T_{max} and T_{min} curves are obtained. The

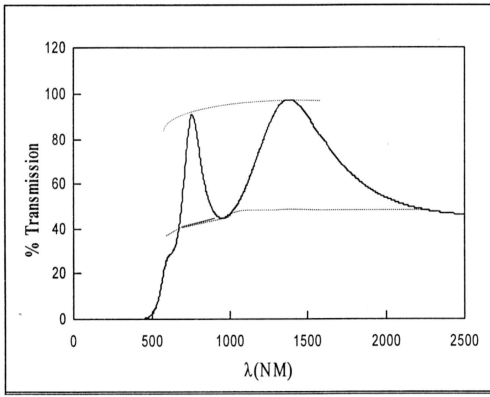

Figure 3.12 A Typical Optical Transmission Spectrum with an envelope

optical thickness can be deduced from the fringe pattern of the transmission spectrum. The basic equation for interference fringes to occur has already been discussed in equation (2.51) and (2.52), namely

$$2nd = m\lambda \quad \text{and},$$

$$2nd = \left(m + \frac{1}{2} \right) \lambda$$

where 'm' is the order for the extremes and has the value of an integer or for a maxima and half integer for a minima. The refractive index of the sample is determined using the following equation,

$$n = \left[N + \left(N^2 - n_0^2 n_1^2 \right)^{\frac{1}{2}} \right]^{\frac{1}{2}} \tag{3.17}$$

where

$$N = \frac{\left(n_0^2 + n_1^2 \right)}{2} + 2 n_0 n_1 \left[\frac{\left(T_{max} - T_{min} \right)}{T_{max} \cdot T_{min}} \right] \tag{3.18}$$

Where, n_0 is the refractive index of air (1.00), n_1 is the refractive index of quartz (=1.55). After calculating for the refractive indices at the extremes, these values are then used to determine the film thickness by using this expression

$$d = \frac{\left[M \lambda_1 \lambda_2 \right]}{2\left[\lambda_2 n(\lambda_1) - \lambda_1 n(\lambda_2) \right]} \tag{3.19}$$

where M is the number of oscillations between two extrema occurring at λ_1 and λ_2 and $n(\lambda_1)$ and $n(\lambda_2)$ are the refractive indices at λ_1 and λ_2 respectively. Equation (3.19) is sensitive to any errors in the values of refractive index (n) and hence is not quite accurate. To minimize this inaccuracy, averaging is done for all values of the thickness. This value is then multiplied by refractive index (n) values to determine the order (m) number for the extremes by using equation (2.51) where this technique were proposed by E.A.Davis et.al [53]. The accuracy is increased by taking the exact integer or half integer value of m, where m increases by 0.5 which occurs only at the extrema values. By using the correct m and values of n, the thickness is again

calculated at the wavelength with the highest transmission. An improved value of refractive index (n) can now be calculated by using this thickness. The n values so obtained can now be fitted to the Cauchy formula and is given by,

$$n = [a / \lambda^2] + b \tag{3.20}$$

Where a and b are constants and were calculated by using the regression method of the Lotus software. If the measured refractive indices were sufficiently accurate at different wavelengths, they would satisfy Cauchy's equation. This fact has actually been verified in this work. The transmission verses wavelength graphs of the sample annealed at different temperatures were obtained. The transmission spectrum of the a-Si:H film is also used to determine the optical band gap of the film material. The absorption coefficient α is calculated using the equation (3.21) the derivation of which was explained earlier in the chapter II (see equation 2.50), which could be rewritten as,

$$\alpha = \frac{1}{d} \ln\left\{\frac{1}{X}\right\} \tag{3.21}$$

where d is the film thickness. X is derived from the expression for transmission, T through air-film-substrate interface as given by Brodsky [54]

$$T = \frac{(1-R_1)(1-R_2)(1-R_3)e^{-\alpha d}}{(1-R_2R_3)\left[1-\left(R_1R_2+R_1R_3(1-R_2)^2\right)e^{-2\alpha d}\right]} \tag{3.22}$$

where R_1, R_2 and R_3 are the reflectivities at the air-film, film-quartz and quartz-air surfaces respectively. Bahl's relations [55] are used to determine the reflectivities.

$$R_1 = \frac{(n_f - 1)^2}{(n_f + 1)^2} \tag{3.23}$$

$$R_2 = \frac{(n_f - n_s)^2}{(n_f + n_s)^2} \tag{3.24}$$

$$R_3 = \frac{(n_s - 1)^2}{(n_s + 1)^2} \tag{3.25}$$

Where n_s is the refractive index of the substrate and n_f is the refractive index of the film. The refractive index of air is 1.0. The following constants are substituted into the equation (3.22).

$$A = (1-R_1)\,(1-R_2)\,(1-R_3) \tag{3.26}$$

$$B = R_2R_3 \tag{3.27}$$

$$C = R_1R_2 + R_1R_3(1-R_2)^2 \tag{3.28}$$

Thus the equation (3.22) can be written in amore simplified form

$$T = \frac{Ax}{(1-B)(1-Cx^2)} \tag{3.29}$$

which can be written in the quadratic form

$$(TC - TBC)x^2 + Ax - (T - TB) = 0 \tag{3.30}$$

which gives a solution of

$$X = \frac{-A \pm \sqrt{A^2 + 4T^2C(1-B)^2}}{2TC(1-B)} \qquad (3.31)$$

The absorption coefficient was calculated at different wavelengths. To estimate the optical energy gap of the material we make use of the equation (2.60) namely,

$$\sqrt{\alpha E} = \sqrt{A}(E - E_g).$$

In other words the optical gap is deduced from the Tauc's plot i.e from the extrapolation of $(\alpha\hbar\upsilon)^{\frac{1}{2}}$ versus $h\upsilon$. The above graph would yield a straight line. The linearity of the straight line is however limited over a small energy range. By dividing the intercept of the linear portion by its slope one can easily estimate the optical energy gap.

3.8.3 Calculation of Hydrogen Content:

We have already discussed in equation (2.62) that by plotting $(n^2-1)^{-1}$ as a function of E^2 one should get a straight line. But in practice the graphs are only linear over a restricted region. We only use the linear portion of the curve for our measurement. From the slope and intercept of the curves it is possible to calculate the dispersion energy E_d and the oscillation energy E_0. Having known the dispersion energy E_d the hydrogen content 'C_H' was calculated using the equation (2.64). The effective valence electron per anion N_V was also calculated by virtue of our knowledge of hydrogen content and is given by

$$N_V = 0.0143 \frac{E_d^2}{E_0 - 1} \times 10^{23} cm^{-3} \qquad (3.32)$$

Where E_0 = (Static refractive index)^2

The results of the various parameters like refractive index, thickness of the sample, Optical gap, hydrogen content and the effective valence electron per anion were calculated in this work and the results are tabulated in the next chapter.

3.9 Annealing Process:

Annealing is a process in which a substance is heated at a particular temperature in a furnace for a specific time and cooled slowly to room temperature in the presence of an inert gas or ambient nitrogen to prevent oxidation of the sample. In this work, the annealing was carried out using the carbolite model. The furnace was first calibrated to determine the position of the sample. The sample was annealed at 100°C, 200°C, 300°C, 400°C, and 500°C for one hour under a steady flow of ambient nitrogen gas at 10sccm to avoid oxidation of a-Si:H. The sample was then allowed to cool down in the furnace with a continuous flow of ambient nitrogen gas to room temperature. Figure 3.13 shows the experimental arrangement for the annealing process. After annealing at each temperature the effect of annealing on the optical and electrical properties of the sample was studied as already explained. Also the photo and dark conductivity of the sample annealed at different temperatures was studied.

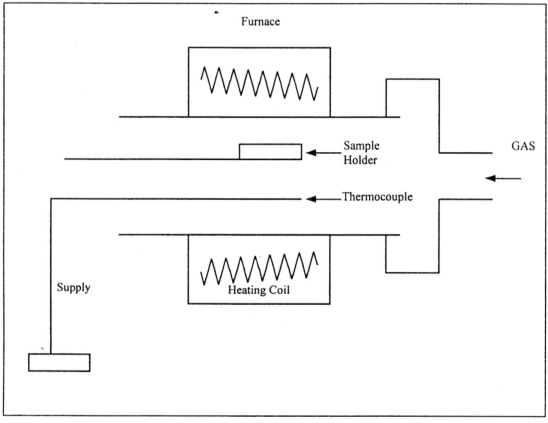

Figure3.13 Experimental arrangement for annealing process